J Gales, L A Bisby, C MacDougall, K MacLean, "Transient high-temperature stress relaxation of prestressing tendons in unbonded construction", Fire Safety Journal, 44(4), pp. 570–579, 2009.

TRANSIENT HIGH-TEMPERATURE STRESS RELAXATION OF PRESTRESSING TENDONS IN UNBONDED CONSTRUCTION

J. Gales[1], L.A. Bisby[2], C. MacDougall[1], and K. MacLean[3]

[1] Department of Civil Engineering, Queen's University, Kingston, Canada
[2] BRE Centre for Fire Safety Engineering, University of Edinburgh, Scotland
[3] Reid Jones Christofferson Inc, Toronto, Canada

Abstract

Unbonded post-tensioned (UPT) flat plate concrete slabs are popular for modern continuous multiple bay floor assemblies due to economic and sustainability benefits (reductions in slab thickness and building self-weight) and structural advantages (decreased deflections over larger spans). Only limited research has been conducted on the performance of UPT flat plate slabs under fire conditions, yet the inherent fire endurance of these systems is sometimes quoted as a benefit of this type of construction. One concern for these structures in fire is that high temperature stress relaxation of the unbonded prestressed reinforcement may cause considerable and irrecoverable prestress loss, with subsequent structural consequences. This paper uses a computational model which has been developed to predict the transient high temperature stress relaxation (i.e., prestress loss) for typical UPT multiple span flat plate slabs in fire, to study the potential prestress relaxation behaviour under various plausible temperature conditions as might occur during exposure to a standard fire. The model is validated using experimental data from relaxation tests performed on locally heated unbonded seven-wire prestressing stand. The initial prestress level, concrete cover to the prestressed reinforcement, and ratio of heated length to overall tendon length are varied to investigate the potential implications for prestress loss, and subsequently for flexural and punching shear capacity. The results highlight the need for particular care in the construction of UPT slabs to ensure adequate concrete cover for structural fire safety.

Keywords: Prestressing steel; post-tensioned slabs; high temperature creep; stress relaxation; unbonded construction; residual capacity; fire endurance

1. Introduction and Objectives

Unbonded post-tensioned (UPT) flat plate slabs are favoured in modern continuous multiple bay floor assemblies due to economic and sustainability benefits (reduction of building weight by eliminating floor beams and reducing slab thickness) and structural advantages (increased span to depth ratios and excellent deflection control). However, only very limited research has been performed on the behaviour of realistic UPT slabs in fire. Of particular interest in the current paper is the potentially problematic high temperature creep (or relaxation) behaviour of UPT strands in multiple bay structures when subjected to standard fire conditions. The mechanical properties of prestressing steels are well known to degrade under high temperatures, and under certain conditions this may result in dramatic and irrecoverable loss of prestress [1], with subsequent consequences for the load carrying capacity of the structure.

Expanding on prior experimental research aimed at studying the high temperature stress relaxation of prestressing strands locally exposed to elevated temperatures [2], a simple computational model was developed to provide a rational prediction of prestress loss (or tendon stress variation) both during and after fire in UPT flat plate concrete structures. The model is used herein to perform parametric studies on the effects of various key parameters on prestress loss during exposure to a standard fire, and to highlight potential concerns and areas where additional study is warranted. It should be noted at the outset that only the prestressing tendons are considered in the current study, and the surrounding structure is assumed not to deform due to the fire. Clearly, this is a dramatic over simplification of reality – one which will be remedied in future work – since thermal deformations (e.g., thermal bowing), continuity, membrane action, and restraint are all known to play significant roles in the fire performance of real, multiple bay continuous concrete slabs. Furthermore, fire tests on bonded prestressed concrete double tee beams [3] have shown that tendon stress increases up to 250 MPa may occur due to thermal bowing in the early stages of a fire; these potential tendon stress increases during the initial stages of fire have also been ignored in the current analysis.

2. Research Significance and Background

Two significant effects of fire can cause a reduction of prestress force in an UPT tendon; namely a gradual, recoverable reduction of prestressing force resulting from restrained thermal expansion, and a more severe, irrecoverable reduction resulting from creep (or relaxation) under stress at high temperatures. Because creep is a time-stress-temperature dependent process, a complex interaction exists between prestress levels and temperature history for a tendon which undergoes a localized heating and cooling cycle. Creep is typically so small as to be negligible for prestressing steel under ambient service conditions. However, under stress and at temperatures specific to cold drawn prestressing strand, irrecoverable creep will accelerate and cause a relaxation of prestress. This will affect the capacity of UPT flat plate slabs in both flexure and punching shear, both of which are functions of the slab geometry, concrete strength, amounts of mild and prestressed steel reinforcement, and prestressing force.

Realistic large-scale tests on structures in fire are rarely feasible, which necessitates the use of computational models to aid in the evaluation of the structural effects of a severe building fire. Indeed, in some forward-looking jurisdictions complex numerical models are currently used to perform performance-based structural design for fire safety. However, only limited research, experimental or computational, is available on the capacities of UPT flat plate slabs either during or after fire. An excellent summary of prior work in this area has been presented previously by Lee and Bailey [4], and additional recent furnace tests have also been reported by Ellobody and Bailey [5] and Kelly and Purkiss [6], although in both cases these have been isolated member tests and the unbonded tendon lengths were therefore unrealistic. This paper represents the first attempt to consider the potential consequences of localized heating of unbonded prestressing strands in fire; an important first step towards rationally modelling the complex behaviour of real UPT flat plate structures in fire.

3. Modelling Transient Thermal Creep and Stress Relaxation at High temperature

A simple computational model for predicting prestress loss in UPT tendons in concrete flat slab structures during fire (accounting for transient thermal creep and stress relaxation) was programmed in Fortran. Fundamentally, the model focuses on the calculation of the transient high temperature thermal creep strain increment over a chosen length of tendon at constant temperature (i.e. a predefined thermal region) during a given time interval, and then on determining the overall relaxation of stress for an unbonded tendon over its total length by summing the contributions from the various thermal regions along the length of the tendon; these regions may be at different temperatures. The change in strain in each thermal region thus directly affects the change in overall prestress level through the invocation of a temperature-dependent modulus of elasticity, which also varies along the length of the locally heated tendon.

Two main input data files are required; namely discretized heated coordinates along the tendon's length (i.e., a numerical description of the tendon's geometry and depth profile within the concrete slab), and the corresponding time-temperature histories during fire at various depths of concrete cover (which can be obtained experimentally, by standard heat transfer analysis, or from design tables). These two sets of information are subsequently used to develop (by interpolation) time-temperature histories for any chosen thermal region along the length of the tendon.

In the absence of test data on the time-temperature histories of a tendon during fire, a simple heat transfer algorithm can be used to calculate spatial and temporal variations in temperature through a flat concrete slab using a finite difference elemental energy balance approach. The current analysis uses a model which accounts for variations in the thermal properties of the concrete and moisture evaporation and which was coded and validated previously [7]. Note that the presence of steel reinforcement is assumed not to influence the heat transfer behaviour, an approach which is considered valid for bonded steel reinforcement but which may or may not be conservative for UPT tendons within a duct.

Once the thermal history of the tendon at various depths is known, the longitudinal thermal profile at any given instant in time can be compiled based on user-specified longitudinal coordinates at discrete locations along the tendon. The model uses these longitudinal coordinates to discretize the tendon into regions of uniform constant temperature. The length and location of the longitudinal regions remain unchanged during the analysis. In this manner, the tendon is discretized into *thermal regions* rather than physical elements – a concept that is important in understanding the procedure used for transient prestress loss calculations described below. For draped parabolic tendons, the model's accuracy is affected by the longitudinal tendon discritization, with greater accuracy for shorter thermal regions, since the tendon temperature varies continuously with concrete cover.

The analysis has been developed to enable consideration of either large scale or localized fires over any portion of a continuous multiple bay structure. A portion of the tendon that is outside the heated region (i.e. in adjacent bays of a multiple bay structure) is assumed to remain at ambient temperature. Longitudinal heat transfer along the tendon is therefore assumed to be insignificant. The overall stress-relaxation algorithm is based on an extension of previous work by MacLean [2], although the version described in the current paper allows for a more rigorous and versatile analysis of data using adaptive tendon discretization and finer longitudinal thermal regions. The algorithm incorporates analytical models and coefficients from several prior studies (described below) to formulate a stress-relaxation model capable of approximating the change in tendon stress as a result of any transient heating and cooling regime for any overall tendon length, heated length, tendon profile, concrete cover, and initial prestress level (but, importantly, ignoring interactions with the concrete).

Two main functions are involved; one which increments time and another which treats the analysis of each thermal region for each time step separately, and then determines the global change in tendon stress for the current time step. For each thermal region during a given time step, the analysis is performed as shown in Figure 1. Upon completion of the time step, an average stress relaxation is calculated over the length of the tendon (this is a global prestress loss because the tendon is unbonded) and the prestress is updated for use as the initial stress in the subsequent time step. During each time step and for each thermal region, the thermal strain, ε_T, is determined on the basis of thermal expansion of the prestressing steel using Equation 1 [8]:

$$\varepsilon_T = -2.016\times10^{-4} + 1.0\times10^{-5}T + 0.4\times10^{-8}T^2 \text{ for } 20°C < T < 1200°C \quad (1)$$

where T is the temperature in degrees Celsius. The model considers the current and previous temperatures of the particular thermal region to calculate the change in thermal strain, $\Delta\varepsilon_T$, during the time step. Clearly, increases in temperature will contribute to prestress loss for a tendon of fixed overall length. This component of prestress loss is reversible upon cooling, whereas creep at high temperature, and the related relaxation induced during heating (and cooling) events, causes additional, irreversible prestress (tendon stress) loss [9].

Creep strains in various grades of steel at high temperature can be approximated using Harmathy's pioneering research in this area [10], along with guidance from additional sources [11,12]. Equation 2 [10] can be used to compute the creep strain, ε_{cr}, at a given stress and temperature during a finite time interval.

$$\varepsilon_{cr} = \frac{\varepsilon_{cr,0}}{\ln 2}\cosh^{-1}(2^{Z\theta/\varepsilon_{cr,0}}) \text{ for } \sigma \text{ constant} \tag{2}$$

The above is dependent on the *Zener-Hollomon parameter, Z*, which is described below, and a *dimensionless creep parameter*, $\varepsilon_{cr,0}$, which was originally derived by plotting experimental creep strain data versus *temperature compensated time*, θ. Temperature compensated time is described using an Arrhenius equation such as Equation 3 [13]:

$$\theta = te^{\frac{-\Delta H}{RT}} \tag{3}$$

where the temperature, T, is in degrees Kelvin, the length of the current time interval, t, is in hours, and the constant, $\Delta H/R$, which represents the activation energy required to cause molecular motion, is taken as 30556°K [13]. This is based on an approach outlined by Dorn [14] that assumes that the steel behaves like a Newtonian liquid with high viscosity; as temperatures increase the average oscillations of atoms also increase, thus promoting creep by more frequent stress-driven molecular rearrangements.

Haramthy and Stanzak [13] found, by testing Grade 1725 prestressing steel up to 690 MPa, that the *Zener-Hollomon parameter* (also called the *creep phase parameter*) and *dimensionless creep parameter* could be described using Equations 4a, 4b and 5, respectively.

$$Z = 195.27\times10^{6}\sigma^{3} \quad \text{for } \sigma \le 172 \text{ MPa} \tag{4a}$$

$$Z = 8.21\times10^{13}e^{0.0145\sigma} \text{ for } 172 < \sigma \le 690 \text{ MPa} \tag{4b}$$

$$\varepsilon_{cr,0} = 9.262\times10^{-5}\sigma^{0.67} \tag{5}$$

where, σ represents the current stress (in MPa) in a given thermal region (i.e. the total tendon stress at the current time). Prestress loss is calculated in the numerical model by using the creep parameters calculated based on the stress and temperature at the end of any given time step. By using the values of θ in Equation 2 at the start and end of the current time step, the difference in creep strain during the time step can be calculated for each thermal region.

Following the computation of transient thermal creep in the individual thermal regions of the tendon during a time step, the total strain change for each region can be computed by summing thermal and creep strain increments. Since the total elongation of the tendon is assumed constant, this dictates that an increase in creep and/or thermal strain will be proportionally followed by a decrease in strain to cause stress, which leads to Equations 6a and 6b for the change in strain to cause stress in a given thermal region during a time step.

$$\Delta\varepsilon_{Total} = 0 = \Delta\varepsilon_{\sigma}(\sigma) + \Delta\varepsilon_{T}(T) + \Delta\varepsilon_{cr}(\sigma,T,t) \tag{6a}$$

or

$$\Delta\varepsilon_{\sigma}(\sigma) = -\left(\Delta\varepsilon_{T}(T) + \Delta\varepsilon_{cr}(\sigma,T,t)\right) \tag{6b}$$

where $\varepsilon_{\sigma}(\sigma)$, $\varepsilon_{T}(T)$, $\varepsilon_{cr}(\sigma,T,t)$ are the strains due to mechanical stress, thermal expansion, and creep, respectively. Thermal and creep strain changes for each thermal region are then converted to a change in stress using a temperature dependent modulus of elasticity determined based on a regression analysis of data presented by Ruge and Winklemann in Anderberg (Equation 7) [1,2]:

$$\frac{E_T}{E_{20°C}} = -2\times10^{-6}T^2 + 0.2\times10^{-6}T + 0.987 \tag{7}$$

where E_T is the modulus of elasticity at a given temperature, *T*, in degress Celsius, and $E_{20°C}$ is the modulus of elasticity at 20°C. Stress changes from each thermal region are averaged over the length of the tendon and the resulting overall average change in tendon stress (stress relaxation) is applied to the stress at the beginning of the time step, such that the tendon's overall elongation remains unchanged. The time is then incremented forward and the process is repeated (using the same thermal regions). This implies that the prestressing tendon physically moves through the heated regions as it locally expands and contracts during the analysis, whereas the heated regions remain stationary.

The computational model's output is the time-history of prestress for the tendon. Because under very short heated lengths the tendon may physically tear itself apart in the heated region, the program is limited to terminate when a thermal region undergoes a rapid exponential increase in strain (as E_T approaches zero in any stressed and heated region), which is an indication of tendon rupture. This is physically akin to the process of torch-cutting of strands during the fabrication of pretensioned concrete elements in a precasting plant – the extreme case of localized heating causing transient creep and prestress relaxation.

The reader will note that the current model is essentially linear elastic in the way in which it treats changes in mechanical strain causing stress. This is appropriate only for cases, such as the current analysis, where the stress in the tendon remains sufficiently low that the tendon is indeed behaving in a linear elastic manner in response to instantaneous changes in stress. The yield strength and elastic modulus of prestressing strand will decrease as the temperature of the strand increases. For example, Eurocode 2: Design of concrete structures – Part 1-2: General rules – Structural fire design [15], provides simple equations that can be used to approximate the reduction in tensile strength and modulus for prestressing steel with temperature. It is therefore conceivable that the ultimate tensile strength (failure stress) of the tendon might be exceeded within a heated region for a locally heated tendon, and that this loss in strength could result in tendon failure *before* sufficient creep (relaxation) has occurred to reduce the tendon stress to a value less than its strength. In the current study, the stress in the tendon at any given time and temperature was compared against the tensile strength of the tendon at that temperature (using data suggested by Hertz [16]) for every analysis case under consideration; it was determined that the strength never fell below the stress in the tendon, even within the locally-heated region. It is not clear if creep will always outweigh loss of tensile strength at high temperature (indeed they are not independent parameters) but this would be an interesting topic for future study.

4. Testing and Model Validation

The computational model described above was validated by comparison against experimental data collected previously by MacLean [2,17]. Maclean's tests experimentally characterized the effects of localized heating of a straight unbonded prestressing strand by monitoring prestress loss due to creep and thermal expansion at high temperature in a laboratory setting.

4.1 Summary of MacLean's Experiments

Eight transient high temperature experiments were conducted to quantify the effects of creep and relaxation on 13 mm diameter Grade 1860 ASTM A416-03 low relaxation 7 wire strands pre-stressed to about 55% of

ultimate – typical of service conditions for a UPT slab after both short and long-term loses have accumulated in a real structure [18].

Figure 2, which is adapted from MacLean [17], illustrates the experimental configuration used in these tests. A single strand, 6300 mm in length, was stressed in a prestressing bed using a center hole hydraulic jack and standard chucks, and incorporating two load cells. A custom- built, horizontal, radiant-type electric tube furnace was used to locally heat the strand to predetermined temperatures under various ramp-soak-cool regimes. Seven K-type thermocouples (denoted *TCi* in Figure 2) were used to record temperatures along the strand during heating and to obtain experimental time-temperature histories at selected locations. Load cells at each anchorage were used to measure changes in prestress force during heating and cooling.

The experiments used a heated length of approximately 610 mm at the middle of the tendon and five different temperature set points; 200, 300, 400, 500, and 700°C. A heating ramp phase at 10°C/min was followed by a constant temperature soak phase of either 5, 45, or 90 minutes, and finally a cooling period where the furnace was switched off and the tendon was allowed to cool naturally to ambient conditions. The ramp rate was chosen to be representative of the heating rates which could be expected for prestressing tendons protected by concrete cover and exposed to a standard fire [19]. A 90 minute soak time was selected to be representative of typical fire endurance ratings of required for restrained UPT floor systems with 20 mm of concrete cover. Additional tests were performed to verify repeatability and to study the effects of varying soak time at a given temperature. Full details of these tests are given elsewhere [2,17].

4.2 Computer Program Validation

MacLean's measured longitudinal tendon temperature data [17] were used to compare against the results of the computational model for two different analyses; varying temperature set point levels and varying soak durations. The raw temperature data from seven thermocouples recorded in the experiments were used to discretize the tendon's length into regions of constant temperature by linear interpolation.

Figure 3a compares the measured and predicted prestress variation for a 90 minute soak time at various set point temperatures from 200°C to 700°C. It is clear from this figure that the model is able to accurately but (in general) conservatively predict the prestress variation recorded during Maclean's tests. The computational model predictions differed from experimental results in each run by a maximum of 1% for 200 and 300°C, 14% for 400°C, 21% for 500°C, and 57% for 700°C (although the large variance at 700°C was seen in the cooling phase only). To clearly illustrate the effects of transient creep/relaxation at high temperature, Figure 3b shows a comparison of the model predictions made accounting for creep (black lines) and neglecting creep and including only thermal expansion (grey lines). This was done using MacLean's experimental temperatures for the 300, 500, and 700°C exposures. This figure clearly shows the profound influence of creep on reductions in tendon stress at high temperature, and also illustrates the recoverability of thermal strains and the irrecoverability of creep strains.

Figure 4 compares the observed and predicted prestress variation for tendons heated to 400°C with soak times varying from 5 minutes to 90 minutes. The model predictions are seen to differ from experimental results by 5, 11, and 14% for 5, 45, and 90 minutes respectively. The cooling phase predictions were also found to be reasonably accurate, but less conservative in some cases. Figures 3 and 4 clearly show that heating above 300°C causes considerable (and irrecoverable) prestress loss.

In general, the model captures the trends observed in MacLean's tests [2], although comparison with the test data indicates that minor refinement of the model may be necessary. This is likely due to the initial stress levels used in Maclean's tests (≈1000 MPa) being considerably higher than the stress levels for which the high temperature creep parameters were derived by previous authors (0 to 690 MPa). This necessitated a significant extrapolation of available experimental creep data [10,13], which may not be appropriate. Additional high temperature creep tests on prestressing wire are planned by the authors to obtain the relevant high temperature creep parameters for initial stress levels up to or exceeding 1000 MPa.

5. Parametric Studies

The automated nature of the model facilitates examination of various tendon exposure scenarios, such as would be experienced for UPT members with draped tendons, lower than desired concrete cover to the

prestressed reinforcement (due to misplaced tendons or to localized cover spalling during fire), localized, compartmentalized, or travelling fires, and varying initial prestress levels.

To study the potential effects of various parameters on the loss of prestress in UPT slabs subjected to fire, the model was used to conduct parametric studies on a typical example flat plate slab adapted from design Example 3-37 from the Canadian Prestressed Concrete Institute (CPCI) design manual [20]. Figure 5 shows the configuration of this slab. The parametric study assumed a structure continuous over three interior bays (7700 mm each) and two exterior bays (5200 mm each). A room temperature modulus of elasticity of 200 GPa was assumed for the prestressing tendons. The tendon profile was modelled as parabolic, where b_c in Figure 5 represents the depth of cover at midspan with a default value of 20 mm. The slab was analyzed using the previously described [7] finite difference heat transfer analysis to develop 10 mm long thermal regions along the full length of the tendon, each with individually known time-temperature profiles for assumed exposure to the ASTM E119 standard fire [21] over a given area of slab. The 150 mm thick slab was assumed to be constructed from carbonate aggregate concrete having 5% initial volumetric moisture content at the onset of fire, which from a heat transfer point of view is at the conservative end of the likely moisture content spectrum for an in-service slab in an environmentally conditioned structure. Cover spalling has not been considered, nor has a cooling phase. Cooling behaviour could be studied with the current model to provide an indication of potential residual prestress levels for less severe fires, or for fires which are extinguished sufficiently early that refurbishment of the structure for continued use is possible.

A convergence study demonstrated that for thermal region lengths smaller than 10 mm there was no discernable change in the model predictions. Parametric studies were subsequently conducted to investigate the effects of (1) initial prestress level, (2) concrete cover depth to the prestressed reinforcement, and (3) the ratio of heated length to total tendon length.

5.1 Initial Prestress Level

Figure 6 shows the predicted variation of prestress level resulting from exposure to an ASTM E119 [21] standard fire for the example structure for various initial prestress levels. In all cases it is assumed that the fire is confined to the central bay of the example structure (i.e., the outside bays remain at ambient temperature), and that cover to the prestressed reinforcement is 20 mm at midspan.

It is evident in Figure 6 that the prestressing force initially decreases gradually as a consequence of restrained thermal expansion. This is followed by a more severe prestress reduction once creep losses begin to accumulate (depending on the combined stress-temperature condition). It is interesting to note that during the fire (independent of the prestress level at the onset of fire), all of the prestress level curves converge to a common lower bound. For example, after one hour of fire, any tendon initially stressed above 32% ultimate strength (f_{pu}) (as any tendon almost certainly would be in an in-service UPT structure) is predicted to be at the same stress level (about $0.32f_{pu}$ in this case). Most importantly, Figure 6 clearly shows that this typical example structure would experience prestress losses (across all bays) in the range of 50 to 60% after one hour of localized fire exposure for realistic initial prestress levels in the range of 1000 to 1200 MPa.

5.2 Concrete Cover to the Prestressed Reinforcement

To study the effects of varying concrete cover on prestress loss during fire, the model was again applied assuming that only the central interior bay was exposed to fire. The assumed parabolic tendon profile, which was at a fixed depth of 20 mm over the supports (Figure 5), was modified such that the midspan concrete cover varied between 5 mm and 30 mm, with all other parameters held constant. The resulting predicted prestress losses for an initial prestress of 1000 MPa are shown in Figure 7. Again, the prestress losses are initially influenced predominately by restrained thermal expansion, but the creep strains become dominant once the temperature of the tendon exceeds 300°C. Clearly, this temperature is reached more rapidly in tendons with smaller cover. The importance of achieving adequate concrete covers for fire protection in UPT slab structures is therefore paramount. In particular, for the case of 5 mm cover, localized exponential strain increases were predicted in the most heated thermal region, causing the model to terminate and implying tendon rupture in less than one hour. In the current case, 50% loss of prestress occurs after only 22 minutes of fire exposure for 5 mm concrete cover, whereas this point is reached after 80 minutes if the cover is 25mm.

5.3 Ratio of Heated Length to Total Length of Tendon

Seven analysis configurations were used to study the effects of varying the ratio of heated length (i.e., the length of the slab directly exposed to the ASTM E119 [21] standard fire) to the total length of the tendon. Since multiple bay UPT slabs are increasingly used for multi-storey office and residential occupancies, it is possible that a fire could develop locally (i.e., within a single compartment or over a single bay), over several bays, or even over an entire floor plate. Figure 8 shows the predicted effects of the heated length ratio on prestress loss for the example slab, again with an assumed parabolic tendon profile, a cover of 20 mm at midspan, and initial prestress of 1000 MPa. The fire exposures that were considered included: partial bay (2310 mm, 3850 mm, or 5390 mm of fire exposed slab centered on midspan for only the central bay), full bay (the entire central bay only), multiple bay (two and three internal bays), and entire floor (all five bays). The results indicate that greater heated length ratios contribute to larger overall prestress losses during fire, although the effect is far less important than the cover depth effect. It should be noted that when multiple bays are exposed to fire, the increases in prestress loss as compared with the shorter heated length ratio cases are due predominately to *recoverable* prestress loss resulting from restrained thermal expansion. Somewhat counter intuitively, *irrecoverable* prestress losses are actually less for larger heated length ratios, suggesting that the residual prestress recovered after a fire would be greater in these cases (this is has been confirmed using the model but has yet to be demonstrated experimentally).

6. Potential Consequences

Loss of prestressing (due to fire or to other damage) has potentially serious consequences for the load carrying capacity of a UPT flat plate structure. In particular, both the flexural capacity and the punching shear capacity may be reduced as prestressing force is lost (all other factors being equal). For the purposes of simple illustration, consider the example UPT slab of Figure 5. The width of each design strip in this structure is 6100 mm. To meet the assumed factored load demand for moment and shear under ambient conditions, twelve 13 mm diameter Grade 1860 seven wire tendons (with a parabolic profile as shown) and ten 10 mm nominal diameter grade 400 bars (assumed at 20 mm clear cover) were provided per design strip of slab. Assuming an ASTM E119 [21] standard fire, and considering degradation of mechanical properties of concrete, mild steel and prestressed reinforcement, and prestress loss at elevated temperature, punching shear and positive and negative flexural capacity were calculated using the provisions of CAN/CSA A23.3-04 [22].

It must be reiterated that thermal bowing, global thermal expansion, restraint, and compressive or tensile membrane action of the concrete slab, and frictional effects on the unbonded prestressing tendons have been ignored in this illustrative example. Additional research is needed to refine the evaluation of prestress losses within the computational model and to understand the influence interactions with the concrete and frictional effects on tendon stress over multiple bays from compartmentalized fires. Depending on the boundary conditions of a fire exposed bay, the load capacity of a UPT slab may be considerably increased by the development of membrane in-plane forces [23]. These factors should be considered in future studies.

6.1 Flexural Capacity

Reductions in flexural capacity during fire exposure were considered for both positive and negative bending of the middle interior bay of the design example slab. Degradation of mechanical properties of mild steel reinforcement was considered only for positive bending (mid span), since at the supports flexural steel for moment capacity is located well away from the fire exposed surface. Data presented by Harmathy [24] were used to account for degradation of the mild reinforcement's yield strength at elevated temperature using Equation 8.

$$f_s = (1.57 - \frac{T_{mr}}{526}) f_y \text{ for } T_{mr} > 300°\text{C} \quad (8)$$

where f_y is the room temperature yield strength of the mild reinforcement, assumed to be 400 MPa, and f_s is the yield strength at elevated temperature , T_{mr} . For positive bending, concrete degradation at midspan was

assumed to be negligible, since the compressive zone of concrete is located well away from the fire exposed face; however, concrete degradation was included for negative bending calculations at the supports. Various relationships to model the mechanical properties of concrete as a function of the temperature are available in the literature. In the current study, the relationship given by Hertz [25] was used to reduce the compressive strength of concrete using a reduction factor, κ_1, based on the average elevated temperature of the compressive stress block in the slab, T_c.

$$\kappa_1 = \frac{1}{\left[1 + \frac{T_c}{10000} + \left(\frac{T_c}{1080}\right)^2 + \left(\frac{T_c}{690}\right)^8 + \left(\frac{T_c}{1000}\right)^{64}\right]} \tag{9}$$

The Hertz model [25] is accurate for carbonate aggregate concrete [26] and compares well against models summarized by Buchanan [27] for normal density concrete. The κ_1 coefficient is typically increased in calculations where initial compressive stress is present, which must be overcome before tensile stresses can be invoked to cause micro-cracking and damage at high temperature [25,26]. For example, for initial compressive stresses of 0.25 f'_c a factor of 1.25 may be applied to Equation 9 [26]. This factor has also been conservatively neglected in the current discussion.

The yield strength of prestressing steel f_{py} was also modified using a reduction factor κ_2 to account for reductions at high temperature, also from Hertz and given in Equation 10 [16]:

$$\kappa_2 = 0.2 + \frac{0.8}{\left[1 + \frac{T_p}{100000} + \left(\frac{T_p}{750}\right)^2 + \left(\frac{T_p}{550}\right)^8 + \left(\frac{T_p}{650}\right)^{64}\right]} \tag{10}$$

With temperature distributions through the slab (and hence mechanical properties of constituents) known at a given cross-section, CAN/CSA A23.3-04 [22] code equations were used to approximate the flexural capacity of the UPT flat plate slab in both positive and negative bending. The neutral axis depth at assumed plastic hinges, c_y, were found from Equation 11.

$$c_y = \frac{\phi_s A_s f_s + \phi_p A_p \kappa_2 f_{py}}{\alpha_1 \beta_1 \phi_c \kappa_1 f'_c b} \tag{11}$$

where *A* is the area of reinforcement provided with the subscript *s* denoting mild reinforcement and *p* denoting prestressed reinforcement, *c* denotes concrete, ϕ is a code specific material reduction factor (0.65 for concrete, 0.85 for mild steel, and 0.9 for prestressing steel), *b* is the design strip width of the slab, and α_1 is the ratio of average stress in a rectangular compression block to the specified room temperature concrete strength f'_c (assumed as 30 MPa). The resulting c_y values for each plastic hinge are subsequently used to calculate the stress in the prestressed reinforcement at ultimate limit state, f_{pr}, according to Equation 12, which is adapted from Clause 18.7.2(b) of CSA A23.3-04 [22].

$$f_{pr} = f_{pe} + \frac{8000}{l_o} \sum_n (d_p - c_y) \leq f_{py} \tag{12}$$

where f_{pe} represents the prestress in the tendons after all short and long term losses (including prestress losses due to fire), d_p is the extreme compression fibre to the centroid of the prestressing steel at the location of the plastic hinge, l_o is the tendon length between anchors, and *n* is the number of plastic hinges (3 for an interior span). The compressive stress block depth, *a*, is therefore given by Equation 13:

$$a = \frac{\phi_s A_s f_s + \phi_p A_p f_{pr}}{\alpha_1 \phi_c \kappa_1 f'_c b} \tag{13}$$

Using f_{pr} and considering the contributions from the flexural steel and the concrete, the moment resistance, M_r, can be calculated at each time step using Equation 14:

$$M_r = \phi_p A_p f_{pr} (d_p - \frac{a}{2}) + \phi_s A_s f_s (d_s - \frac{a}{2}) \tag{14}$$

The resulting variations in flexural capacity positive and negative bending are presented in Figures 9 and 10, respectively. These figures consider the variation in concrete cover to the prestressed reinforcement at midspan (5 mm, 15 mm and 30mm) and heated length ratio (7% and 100%). Similar trends are observed for both positive and negative bending. Flexural capacity contours confirm the importance of accurate tendon placement during construction, since moment capacity drops very rapidly (due to complete prestress loss and followed by tendon rupture) for the 5 mm cover case. Fifty percent loss of flexural capacity is predicted in less than 30 minutes in this case, for an otherwise 2 hr fire rated assembly. Note also that the flexural capacity is predicted to be reduced by about 50% after about one hour, even for the as-designed default configuration. This simple illustration shows that additional research in this area is warranted.

6.2 Punching Shear Capacity

Prevention of punching shear failure is a critical consideration in the design of flat plate slabs, yet it has apparently received little or no research attention with respect to the fire performance of these systems, despite anecdotal evidence that punching failures may have occurred during real fires. Punching failures may occur around columns when diagonal tension cracks allow the formation of a truncated cone or pyramid around the column which punches through the slab. In extreme cases, this type of failure can result in disproportionate or progressive structural collapse [28,29].

Using the same example slab (Figure 5), an interior slab-column connection was considered to illustrate the potential consequences of prestress loss due to fire for punching shear. Again, Canadian code recommendations [22] and thermally degraded material properties are used for the illustration. The compressive stress in the concrete at the centroid of the cross section, f_{cp}, is calculated from Equation 15:

$$f_{cp} = P_e \big/ A_c \tag{15}$$

where P_e is the prestress force after all losses (based on f_{pe} and the number of tendons) and A_c is the cross-sectional area of concrete in the design strip. A square column size of 300 mm has been assumed. A shape factor, β_p, is determined based on Equation 16 from Clause 18.12.3.3 in CSA-A23.4-04 [22]:

$$\beta_p = \frac{\alpha_s d}{b_o} + 0.15 \leq 0.33 \tag{16}$$

where d is the average effective depth of the slab, b_o is the perimeter of the critical section of the slab, and α_s = 4 for an interior column. The calculation of b_o assumes the critical punching region to occur at a distance *d/2* from the column face. Using Equations 10, 15, and 16, the punching shear resistance (V_c) around an interior column at each instant in time during fire was calculated using Equation 17, for normal density concrete [22].

$$V_c = \beta_p \phi_c \sqrt{\kappa f'_c} \sqrt{1 + \frac{\phi_p f_{cp}}{0.33 \lambda \phi_c \sqrt{\kappa f'_c}}} b_o d \tag{17}$$

This equation clearly shows that punching shear capacity relies considerably on the prestressing force, highlighting the importance of prestress loss both for fire exposed bays and for adjacent bays which remain at ambient temperature but experience reductions in prestress. The vertical component of the prestressing force was conservatively neglected in this calculation, since the tendon slope is difficult to define and/or control in thin UPT slabs [30]. The resulting predicted variation in punching shear capacity during fire is shown in Figure 11. Again, several different parametric cases are considered. A considerable decrease in punching shear resistance is evident in all cases beyond 30 minutes of fire. At one hour, all but the 30 mm cover contour indicate greater than 30% loss in punching capacity. The 5 mm concrete cover contour indicates about 45% reduction in punching shear capacity in less than one hour, with subsequent tendon rupture.

7. Future Work

The flexural and punching shear capacity reductions presented above are considered by the authors to probably be conservative illustrations (i.e., over-predictions of degradation). While the analysis and comparisons presented in the current paper must be considered preliminary, it is clear that additional research is needed to better understand the fire performance of UPT flat plate systems. Future research by the authors will include experimental determination of creep parameters for prestressing steel at high temperature up to stress levels of 1000 MPa. Further model validation is also planned through high temperature relaxation experiments on locally heated tendons with realistic length and parabolic profiles. Finally, it is important that realistic, full-scale fire tests be performed on loaded multiple bay UPT slabs during fire, both for model development and validation and to ensure that full structure interactions and unforeseen failure modes are properly and rationally accounted for in design.

8. Conclusions

The computational model presented herein allows for reasonably accurate predictions of prestress loss in multiple bay UPT flat plate concrete slabs during fire. The model has been validated against simple high temperature relaxation tests on locally heated straight prestressing strands. Based on the computational model, applied under various parametric scenarios and with the assumptions inherent in the model clearly acknowledged, the following conclusions may be drawn:

- The model indicates that achieving adequate (as specified or greater) concrete covers in regions of positive bending during construction is paramount to maintaining the structural safety of UPT systems during fire. Particular care (and adequate site inspection) is therefore needed during the construction process. Clearly, consideration must be given to spalling during fire, since localized heating of the tendons has structural implications across multiple bays of a UPT structure.
- Parametric studies suggest that the initial prestress level and the heated length ratio are less critical during fire, which suggests that either large (multiple bay) or localised (well-compartmentalized) fires can cause similar reductions in prestress across multiple bays of a structure.
- Simple illustrative calculations performed using extensions of code based equations (modified to account for mechanical degradation of constituent materials and prestress loss due to heating) indicate that there

may be important consequences of fire for UPT structures which are not currently considered in design, both for punching shear and flexural capacity; additional research is therefore warranted.

Acknowledgments

The Authors would like to acknowledge the support of the Natural Sciences and Engineering Research Council of Canada, Queen's University, Dr. T.I. Campbell, and the Canadian Foundation for Innovation.

Notation

a = depth of the compressive stress block of concrete (mm)
A_c = cross-sectional area of concrete (mm^2)
A_s = area of mild steel reinforcement (mm^2)
A_p = area of prestressing steel (mm^2)
α_1 = ratio of average stress in a rectangular compression block
α_s = shape factor coefficient for interior columns
β_1 = compressive stress block factor
β_p = shape factor for punching shear resistance
b = design strip width of the slab (mm)
b_o = effective perimeter of the slab (mm)
c_y = depth of the neutral axis assuming f_{pr} equals f_{pu} (mm)
d_p = depth from the extreme compression fibre to the centroid of the prestressing steel (mm)
d = average depth of the slab (mm)
$\Delta H/R$ = activation energy of creep divided by the Universal Gas Constant (°K)
ε = strain, theoretical creep strain
ε_{cr} = creep strain
$\varepsilon_{cr,0}$ = dimensionless creep parameter
ε_σ = strain due to applied loading and prestress
ε_T = strain due to thermal elongation
E = elastic modulus (MPa)
E_T = elastic modulus at temperature T (MPa)
$E_{20°C}$ = elastic modulus at room temperature (MPa)
f'_c = compressive strength of concrete (MPa)
f_s = degraded yield stress of mild reinforcement due to elevated temperature(MPa)
f_y = yield stress of mild reinforcement(MPa)
f_{cp} = compressive stress in concrete at the centroid of the cross section (MPa)
f_{pe} = tensile strength of prestressing strand/wire after losses (MPa)
f_{pr} = stress in prestressing strand/wire at factored resistance (MPa)
f_{pu} = tensile strength of prestressing strand/wire (MPa)
l_o = anchor to anchor length of tendon (mm)
κ_1 = relative concrete compressive strength reduction factor
κ_2 = relative ultimate prestressing strength reduction factor
σ = stress (MPa)
P_e = applied prestressing force after losses (N)
t = time (hrs)
T = temperature (°C or °K)
T_c = average elevated temperature of concrete compressive zone (°C)
T_{mr} = elevated temperature of reinforcing steel (°C)
T_p = average elevated temperature of prestressing strand (°C)
TC_i = thermocouple temperature (°C)
T_i = thermal region temperature (°C)
V_c = punching shear resistance (Force)

M_r = flexural resistance (kN·m)
n = number of plastic hinges
θ = temperature compensated time (hrs)
ϕ_c = material resistance factor for concrete
ϕ_p = material resistance factor for prestressing reinforcement
ϕ_s = material resistance factor for mild reinforcement
Z = Zener-Hollomon Parameter (hrs^{-1})

References

[1] Anderberg Y. Properties of materials at high temperatures: steel. Rep. No. TVBB-3008 Division of Building Fire Safety and Technology. Sweden: Lund Institute of Technology; 1983.

[2] Maclean, KJN, Bisby, LA and MacDougall, CC. Post-fire assessment of unbonded post-tensioned slabs: Strand deterioration and prestress loss. ACI-SP 255: Designing Concrete Structures for Fire Safety, American Concrete Institute, 10 pp. 2008.

[3] Franssen, JM and Bruls, A. Design and Tests of Prestressed Concrete Beams. Fire Safety Science 1997; 5: 1081-1092.

[4] Lee, DYC and Bailey, CG. The Behaviour of Post-Tensioned Floor Slabs in Fire Conditions. International Congress on Fire Safety in Tall Buildings, Santander, Spain, pp. 183-201, 2006.

[5] Ellobody, E and Bailey, CG. Testing and Modelling of Bonded and Unbonded Post-Tensioned Concrete Slabs in Fire. Fifth International Conference on Structures in Fire, Singapore, pp. 392-405, 2008.

[6] Kelly, F and Purkiss, J. Reinforced concrete structures in fire: a review of current rules. The Structural Engineer, 2008; 86(19): 33-39.

[7] Bisby LA. Fire Behaviour of Fibre-Reinforced Polymer (FRP) Reinforced or Confined Concrete. PhD dissertation, Department of Civil Engineering, Queen's University at Kingston, ON, Canada, 2003.

[8] CEN, Eurocode 2: Design of concrete structures, Parts 1-2: General rules, Structural fire design, ENV 1992-1-2; 1996.

[9] Collins MP, and Mitchell D. Prestressed concrete basics. Canadian Prestressed Concrete Institute, Ottawa ON; 1987.

[10] Harmathy TZ. Deflection and Failure of Steel-Supported Floors and Beams in Fire. Fire Test Methods-Restraint and Smoke 1966 ASTM Special Technical Publication 422, C.C. Carlson, ed., American Society for Testing and Materials, Philadelphia; 1967: 40-62.

[11] Hill AW, and Ashton LA, Fire resistance of prestressed concrete. Civil Engineering (London) 1957; 52(617):1249-1253.

[12] Abrams MS, and Cruz CR, Behaviour at high temperature of steel strand for prestressed concrete. Portland Cement Association – Research and Development Laboratories – Journal 1961; 3(3): 8-19.

[13] Harmathy TZ., and Stanzak, WW. Elevated-Temperature Tensile and Creep Properties of Some Structural and Prestressing Steels. National Research Council of Canada. Division of Building Research, Ottawa, ON; 1970.

[14] Dorn JE, Some fundamental experiments on high temperature creep. J. Mech. Phys. Solids 1955; 3(2): 105-116.

[15] CEN, Eurocode 2: Design of concrete structures, Parts 1-2: General rules, Structural fire design, ENV 1992-1-2; 2004.

[16] Hertz KD. Reinforcement data for fire safety design. Magazine of Concrete Research 2004; 56(8):453-459.

[17] Maclean K. Post-fire assessment of unbonded post-tensioned concrete slabs: strand deterioration and prestress loss. M.Sc thesis, Department of Civil Engineering, Queen's University, Kingston, ON, Canada, 2007.

[18] PTI. Post-Tensioning Manual - Fifth Edition. Post-Tensioning Institute, Phoenix, AZ; 1990.

[19] Kodur VKR, and Bisby LA. Evaluation of Fire Endurance of Concrete slabs reinforced with fiber-reinforced polymer bars. ASCE Journal of Structural Engineering 2005; 131(1): 34-43.

[20] CPCI. Design Manual: Precast and Prestressed Concrete - Fourth Edition. Canadian Precast/ Prestressed Concrete Institute, Ottawa ON; 2007.

[21] ASTM. Standard Methods of Fire Test of Building Construction and Materials. Test method E119-01d, West Conshohocken, PA. American Society for Testing and Materials; 2001.

[22] CSA. Technical Committee on Reinforced Concrete Design. A23.3-04 Design of Concrete structures. Rexdale, Ontario, Canada. Canadian Standards Association; 2004.

[23] Bailey C, Toh, W, and Chan B. Simplified and advanced analysis of membrane action of concrete slabs. ACI Structural Journal 2008; 105(1): 30-40.

[24] Harmathy TZ. Fire safety design and concrete. Concrete design and Construction series. Longman Scientific and Technical, UK; 1993.

[25] Hertz KD. Concrete Strength for fire safety design. Magazine of Concrete Research 2005; 57(8):445-453.

[26] Youssef MA, Motabah M. General stress-strain relationship for concrete at elevated temperatures. Engineering Structures 2007; 29: 2618-2634.

[27] Buchanan A. Structural Design for Fire safety. John Wiley Sons, Chicester; 2001.
[28] Park R, and Gamble W. Reinforced concrete slabs. New York, Wiley; 2000.

[29] Nilson A. Design of prestressed concrete. 2nd Edition, New York, Wiley; 1987.

[30] Ghali A, and Megally S. Design for Punching shear strength with ACI 318-95. ACI Structural Journal 1999; 96(4): 539-549.

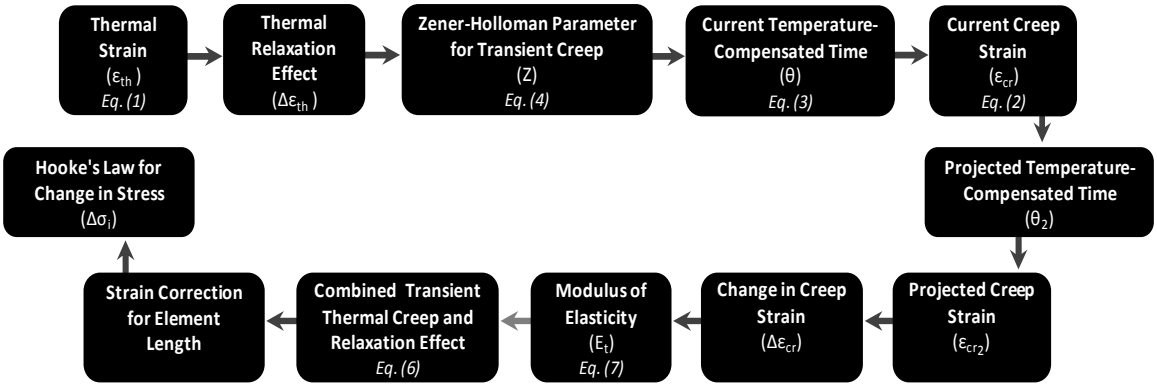

Fig. 1. Computer algorithm for transient thermal creep and stress relaxation model for a constant temperature region during a single time interval

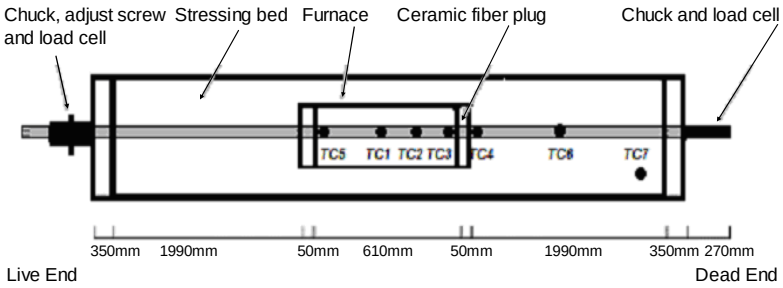

Fig. 2. Schematic plan view of experimental set up used by MacLean [17]

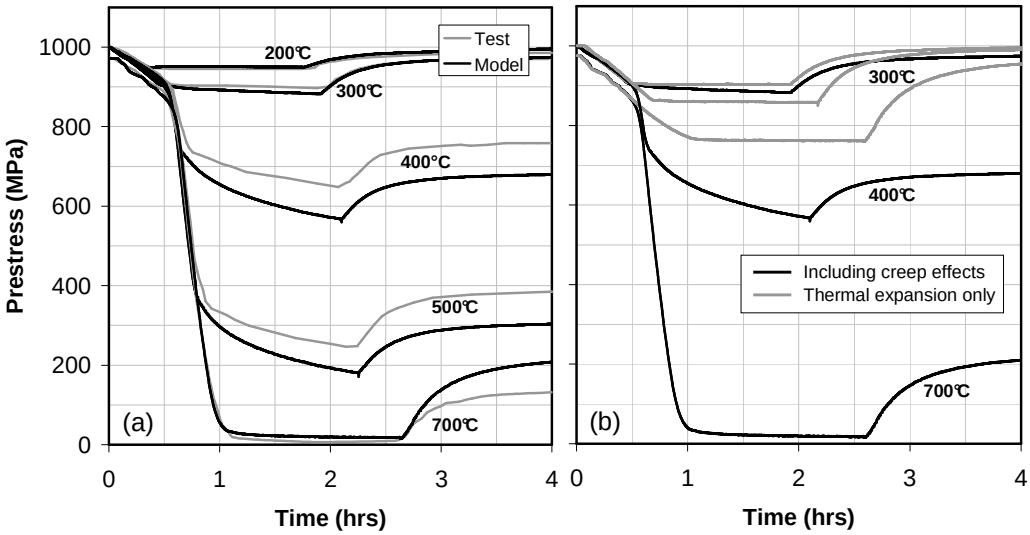

Fig. 3. (a) Predicted and observed results for tendon stress level at various temperature set points and (b) comparison of model predictions incorporating creep against model predictions accounting for thermal expansion only

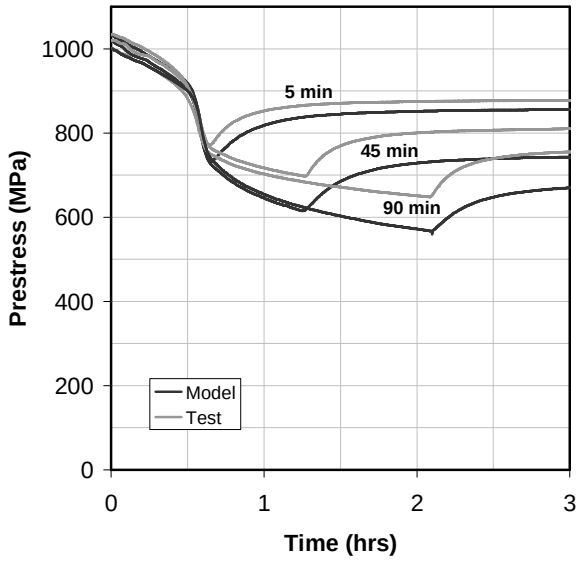

Fig. 4. Predicted and observed stress relaxation using various soak times for a set point of 400°C

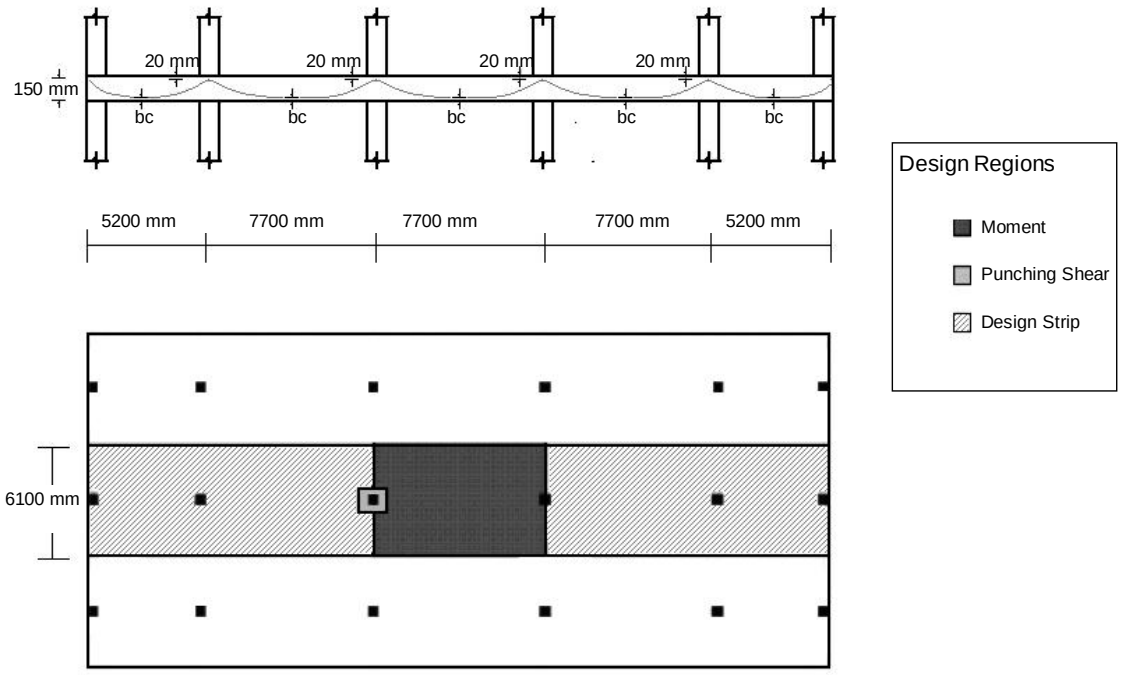

Fig. 5. Schematic section and plan views of the assumed example slab that has been used in parametric analyses

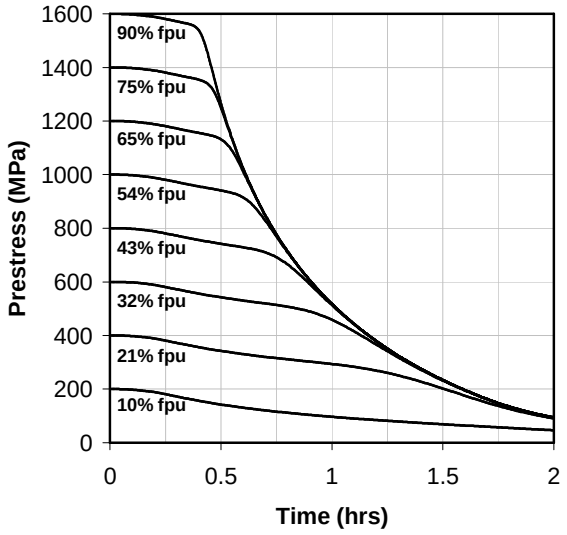

Fig. 6. Effects of varying the initial prestress level on the prestress loss during fire for the example UPT slab subjected to an ASTM E119 [21] standard fire over the central bay

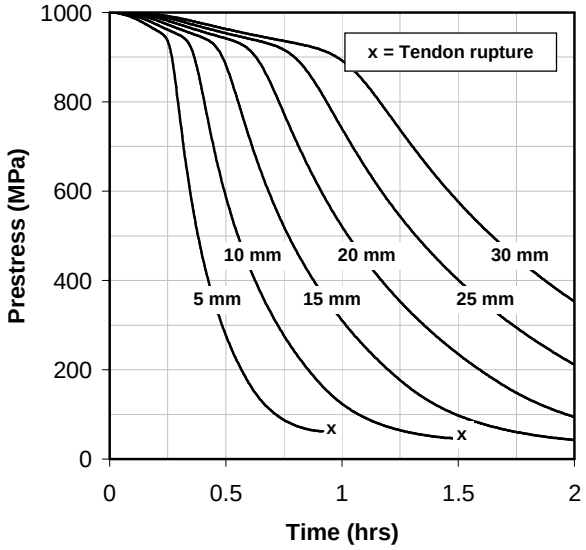

Fig. 7. Effects of varying the concrete cover to the prestressed reinforcement at midspan on the prestress loss during fire for the example UPT slab subjected to an ASTM E119 [21] standard fire over the central bay

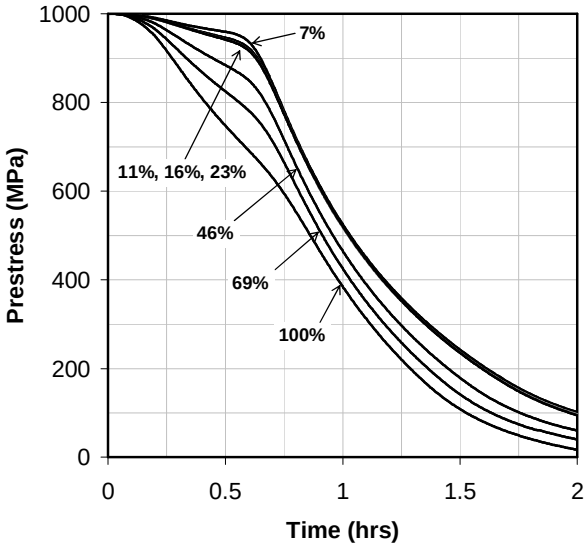

Fig. 8. Effects of varying the ratio of heated length to total tendon length on the prestress loss during fire for the example UPT slab subjected to an ASTM E119 [21] standard fire over the central bay

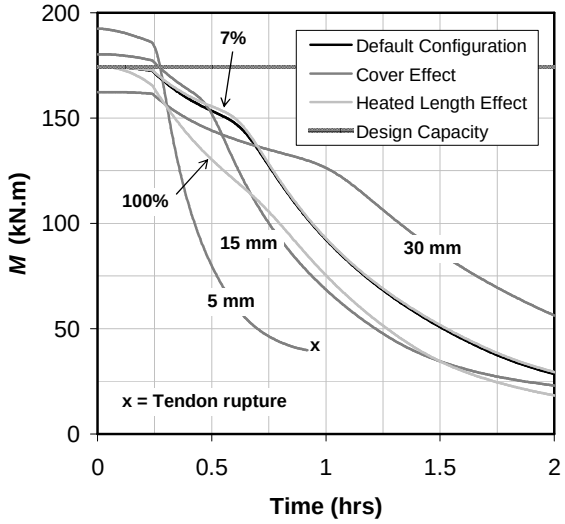

Fig. 9. Predicted variation in positive moment capacity during fire for the example slab with several parameters varied

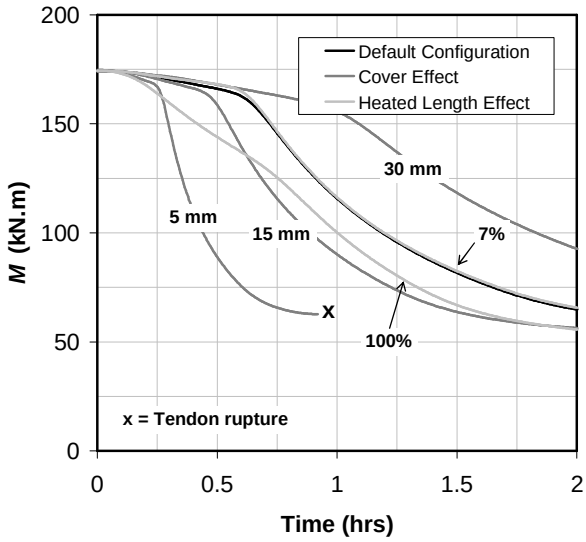

Fig. 10. Predicted variation in negative moment capacity during fire for the example slab with several parameters varied

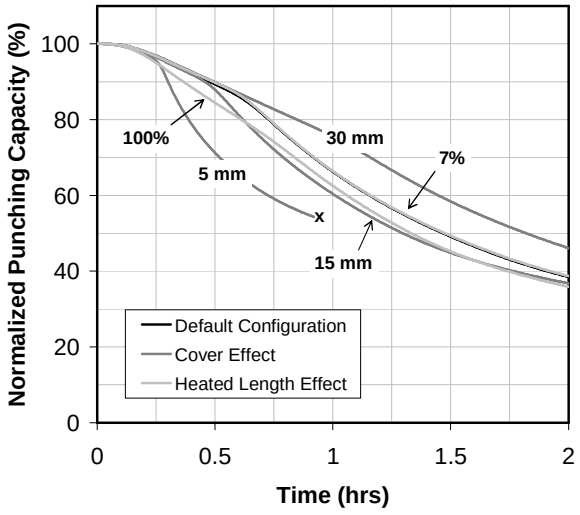

Fig. 11. Normalized predicted variation in punching shear capacity around a 300 mm square interior column during fire for the example slab with several parameters varied

J Gales, L A Bisby, C MacDougall, K MacLean, “Transient high-temperature stress relaxation of prestressing tendons in unbonded construction”, Fire Safety Journal, 44(4), pp. 570–579, 2009.